Contribution from the Laboratoire de Photochimie Générale, ERA du CNRS No. 386, ENSCM, 68093 Mulhouse Cedex, France, Institut de Physique Nucléaire (et IN2 P3), Université de Lyon I, 68622 Villeurbanne Cedex, France, Laboratoire de Chimie Inorganique Moléculaire, Université d'Aix Marseille St. Jérôme, 13397 Marseille Cedex 13, France, and Department of Chemistry and the Saskatchewan Accelerator Laboratory, University of Saskatchewan, Saskatoon, Saskatchewan S7N 0W0, Canada

Xα Method as a Tool for Structure Elucidation of Short-Lived Transients Generated by Pulse Radiolysis or Flash Photolysis. 2. Oxidative Reactions of $PtCl_4^{2-}$

A. GOURSOT,*† H. CHERMETTE,‡ M. CHANON,§ and W. L. WALTZ∥

Received May 2, 1984

Relativistic MS-Xα calculations have been performed on Pt(III) complexes used as models of the transients generated by pulse radiolysis of $PtCl_4^{2-}$ in water or in NaCl neutral and acidic solutions. These structures include the following complexes: (i) $PtCl_4O^{3-}$, $PtCl_4(OH)^{2-}$, $PtCl_5(OH)^{3-}$; (ii) $PtCl_4(OH)_2^{3-}$ or $PtCl_4(OH)(H_2O)^{2-}$; (iii) $PtCl_5^{2-}$, $PtCl_6^{3-}$. The calculated electronic structures and charge-transfer absorption spectra of these d^7 complexes are analyzed, especially in connection with the Pt^{III}–O or Pt^{III}–Cl_{ax} bond lengths. The comparison of the theoretical CT spectra with those obtained experimentally suggests that (i) the short-lived transient, generated by pulse radiolysis of neutral aqueous solutions of $Pt^{II}Cl_4^{2-}$ and absorbing at 450 nm, is best described as $PtCl_4(OH)(H_2O)^{2-}$ or $PtCl_4(OH)_2^{3-}$ and (ii) the transient species observed in neutral or acidic solutions containing an excess of Cl^- anions and absorbing near 290 nm is consistent with the formulation of $PtCl_6^{3-}$ with moderate elongation of the Pt^{III}–Cl_{ax} bond lengths (0.2–0.3 Å). In both cases, only the hexacoordinated models can yield agreement with experimental spectra.

Introduction

The study of short-lived metal complexes where the metal center is formally in an unusual oxidation state has been greatly enhanced by the application of pulse radiolysis techniques. However, because of their transitory existence, a major difficulty occurs in the elucidation of their structures and the correlation of such with reactivity. Theory-based approaches to the study of these transients provide a very valuable tool to help in their structural characterization.

In this context, we have undertaken quantitative evaluations of the charge-transfer (CT) spectra of unstable Pt(III) products formed upon irradiation of aqueous solutions of Pt(II) and Pt(IV) complexes. We have chosen for this purpose the relativistic version of the multiple-scattering (MS) Xα molecular orbital (MO) model, which has been shown in the last few years to give a realistic description of the electronic structure of coordination compounds.[1,2] First, test calculations have been performed on the stable compounds $Pt^{IV}Cl_6^{2-}$[3] and $Pt^{II}Cl_4^{2-}$,[19] leading to reliable descriptions of their ligand field and CT absorption spectra. Then, we have investigated the calculated electronic structures and absorption spectra of different models of Pt(III) transients that could be involved in the reaction of the hydrated electron with $Pt^{IV}Cl_6^{2-}$.[4] The present paper is devoted to the analysis of the possible structures of Pt(III) transients arising from the oxidative reactions of $Pt^{II}Cl_4^{2-}$. The main experimental features to be compared with the calculated results are as follows.

The transient spectrum observed in the pulse radiolysis of $PtCl_4^{2-}$ in neutral aqueous solutions exhibits a maximum at 450 nm at the end of the pulse. This peak decays after about 20 μs and is replaced by another absorption maximum at 410 nm. As already concluded by several authors,[5-7] it is likely that the Pt(III) complex absorbing at 450 nm is obtained directly from the reaction between Pt(II) and OH and that it subsequently converts to another more stable Pt(III) species absorbing at 410 nm. Adams and co-workers[5] have proposed that the nascent short-lived transient is a square-pyramidal pentacoordinated complex of Pt(III), which then transforms into a trigonal-bipyramidal Pt(III) structure, featuring a peak at 410 nm. The same or a similar transient that also absorbs at 410 nm is generated by pulse radiolysis or flash photolysis of aqueous solutions of $PtCl_6^{2-}$. In highly acidic or basic aqueous solutions of $PtCl_4^{2-}$, only transient absorption at 410 nm is observed.

When the neutral solutions of $PtCl_4^{2-}$ contain an excess of Cl^- anions, the shape of the spectrum is unchanged above 350 nm but another peak appears near 260[8] or 290 nm,[7] which depends on the presence and concentration of Cl^- anions. This new peak appears only when the ratio $[Cl^-]/[PtCl_4^{2-}]$ is greater than 100/1. But even when it amounts to 1000/1, the 450- and 410-nm absorptions are only partially suppressed.

In HCl solutions, the situation is markedly changed: when $[Cl^-]/[PtCl_4^{2-}]$ is 100/1, the 450- and 410-nm peaks are absent and the absorption around 260–290 nm is considerably enhanced. The results obtained in neutral and acidic solutions of $PtCl_4^{2-}$ with high concentrations of Cl^- suggest that the oxidizing species is no longer OH but rather the ion radical Cl_2^-, formed by reaction of OH and Cl^-.[7,8] Different proposals have been made for the Pt(III) transient obtained from the reaction of Cl_2^- with $PtCl_4^{2-}$: a planar $PtCl_4^-$ configuration,[7] $PtCl_6^{3-}$, and/or $PtCl_5^{2-}$ structures.[8]

Whatever their chemical natures are, the oxidation of $PtCl_4^{2-}$ to different Pt(III) transients must occur either by direct electron transfer or by addition of the reactive radicals OH or Cl_2^- to the Pt(II) complex. The former mechanism could lead directly to the formation of the square-planar $Pt^{III}Cl_4^-$ transient. The latter oxidative route implies that the attack is on $PtCl_4^{2-}$ along the axis of the fully occupied Pt $5d_{z^2}$ orbital, leading to an increase in coordination number. In fact, the electronic structure of $PtCl_4^-$ has already been investigated and it has been shown that this d^7 complex must have low-energy ligand to metal CT transitions (LMCT) due to the partial occupation of its highest occupied molecular orbital (HOMO).[4] From the comparison of its calculated and experimental absorption spectra, it has been inferred that this Pt(III) species, with possibly weakly coordinating apical chlorines, is responsible for the absorption at 410 nm.

On the basis of these results, it is unlikely that $PtCl_4^-$ is the species absorbing near 290 nm, as proposed by Broszkiewicz et al.[7] It is thus of considerable interest to calculate with sufficient accuracy the charge-transfer spectra of different penta- and

† ENSCM.
‡ Université de Lyon I.
§ Université d'Aix Marseille St. Jérôme.
∥ University of Saskatchewan.

(1) Weber, J.; Geoffroy, M.; Goursot, A.; Penigault, E. *J. Am. Chem. Soc.* **1978**, *100*, 3995.
(2) Goursot, A.; Chermette, H.; Daul, C. *Inorg. Chem.* **1984**, *23*, 305.
(3) Goursot, A.; Penigault, E.; Chermette, H. *Chem. Phys. Lett.* **1983**, *97*, 215.
(4) Goursot, A.; Chermette, H.; Penigault, E.; Chanon, M.; Waltz, W. L. *Inorg. Chem.* **1984**, *23*, 3618.
(5) Adams, G. E.; Broszkiewicz, R. B.; Michael, B. D. *Trans. Faraday Soc.* **1968**, *64*, 1256.
(6) Ghosh-Mazumdar, A. S.; Hart, E. J. *Int. J. Radiat. Phys. Chem.* **1969**, *1*, 165.
(7) Broszkiewicz, R. K.; Grodkowski, J. *Int. J. Radiat. Phys. Chem.* **1976**, *8*, 359.
(8) Storer, D. K.; Waltz, W. L.; Brodovitch, J. C.; Eager, R. L. *Int. J. Radiat. Phys. Chem.* **1975**, *7*, 693.

0020-1669/85/1324-1042$01.50/0 © 1985 American Chemical Society

Table I. Electronic Energy Levels[a] and Charge Distribution for $PtCl_4O^{3-}$

MO	energy, Ry	Pt							Cl_{eq}			O			int	out
		s	p_z	$p_{x,y}$	d_{z^2}	$d_{x^2-y^2}$	d_{xy}	$d_{xz,yz}$	f	s	p_σ	p_π	s	p_σ	p_π		
$6a_1$	−0.145		5		27				1		2	2	1	27		28	7
6e	−0.248							23	1		1				58	16	1
$2b_2$	−0.324						71					19				9	1
5e	−0.368							43				30			16	10	1
$1a_2$	−0.444											90				9	1
4e	−0.481			1					1		86					9	1
$3b_1$	−0.488								1			86				12	1
$5a_1$	−0.511	7			37						1	3	2	42		7	1
$4a_1$	−0.528		1		1							77	1	3		16	1
3e	−0.556			5				5			67	12				9	2
2e	−0.567			1				21			15	43			5	14	1
$1b_2$	−0.610						22					62				15	1
$2b_1$	−0.674					38				1	59						2
$3a_1$	−0.689	13			13					3	68					2	1
$2a_1$	−1.362		1		4					13			78			4	
1e	−1.364			2					1	95						2	
$1b_1$	−1.366									94						2	
$1a_1$	−1.403	4								79	1		12			4	

[a] The highest occupied level is $6a_1$, which accommodates one electron.

hexacoordinated Pt(III) species so as to be able to compare the results with the observed peaks at 450 nm and 290 or 260 nm. With this objective, we have examined in this report the calculated absorption spectra of the following complexes: (i) $PtCl_4O^{3-}$, $PtCl_4(OH)^{2-}$, $PtCl_5(OH)^{3-}$; (ii) $PtCl_4(OH)_2^{3-}$ or $PtCl_4(OH)(H_2O)^{2-}$; (iii) $PtCl_5^{2-}$, $PtCl_6^{3-}$.

We have considered basically square-pyramidal models (C_{4v}). The trigonal-bipyramidal form (D_{3h}), which could be deduced from the C_{4v} structure by Berry rotation, has already been investigated for $PtCl_5^{2-}$.[4] In this case, both structures lead to calculated CT transitions in the UV region. A C_{4v}–D_{3h} interconversion cannot thus be put forward to interpret the experimental absorptions observed in the 400–500-nm region of the spectra.

Elongations of the axial bond lengths have been generally considered to take account of the electronic repulsion between the metal and the axial ligand(s) caused by the occupation of the σ-antibonding HOMO. As the true Pt^{III}–Cl or Pt^{III}–O bond lengths are unknown, the use of a standard maximum elongation has been used to analyze the influence of the axial bond length upon the CT absorption spectrum.

Computational Method

An OH^- or H_2O ligand has been modeled as an oxygen sphere containing 10 electrons. The Pt–O distance has been taken as 3.855 au (2.04 Å), corresponding to the experimental value in $Pt(OH)_6^{2-}$.[9] The value of 4.388 au (2.32 Å) has been used for elongated Pt–O bond lengths. A value of 4.388 au has been chosen for the Pt–Cl bond lengths, as determined experimentally for $PtCl_4^{2-}$.[10] Standard values have been used for the Pt–Cl_{ax} bond length elongations: 0.4 and 1 au for $PtCl_5^{2-}$, 0.4 au for $PtCl_5O^{4-}$, 0.2 and 0.4 au for $PtCl_6^{3-}$.

When a sixth coordinating Cl^- anion is considered, its distance to Pt has been set equal to 5.388 au. The calculations have been performed in C_{4v} symmetry, except those for $PtCl_4O_2^{5-}$ and $PtCl_6^{3-}$ (D_{4h}). The C_4 axis of symmetry is collinear to the z axis, and the $z0x$ and $z0y$ planes are σ_v mirrors.

The radii of Pt and Cl atomic spheres are the same as those used in the $PtCl_6^{2-}$ case[3] (R(Pt) = 2.561 73 au and R(Cl) = 2.70607 au). The radius of the oxygen sphere (2.064 au) has been determined by the requirement of having the same overlap with platinum as that of the axial chlorine. An external tangent outer sphere is used in each case. It also serves as a Watson sphere[11] on which a positive net charge of 2+ ($PtCl_5^{2-}$), 3+ ($PtCl_6^{3-}$), 4+ ($PtCl_5O^{4-}$), or 5+ ($PtCl_4O_2^{5-}$) is distributed to simulate the environment of the complex anion. The values of the exchange parameters of platinum (α_{Pt} = 0.693 06), chlorine (α_{Cl} = 0.723 25), and oxygen (α_O = 0.744 47) are those optimized by Schwartz.[12] A weighted average of these atomic values is chosen for the α value of the interatomic and extramolecular regions. In all calculations, partial waves up to l = 4 are included in the multiple-scattering expansions in the metal sphere and the extramolecular region and partial waves up to l = 1 in the chlorine and oxygen spheres. The transition-state procedure[13] is used for the determination of the excitation energies, without the inclusion of spin polarization.

Electronic Structures of Pt(III) Models

All the studied structures are related to the basic models $PtCl_4O^{3-}$ (for $PtCl_4O^{3-}$ or $PtCl_4OH^{2-}$), $PtCl_4O_2^{5-}$ (for $PtCl_4(OH)(H_2O)^{2-}$ or $PtCl_4(OH)_2^{2-}$), and $PtCl_5^{2-}$. We first describe their electronic structures and then compare their main features. All of these species are d^7 complexes with $^2A_1$ ground states. The singly occupied HOMO corresponds to σ-antibonding interactions of the Pt $5d_{z^2}$ atomic orbital (AO) with the p_z AO of the axial ligand(s).

(1) $PtCl_4O^{3-}$. The valence levels of this model, calculated for a standard geometry (model A), are reported in Table I. The HOMO exhibits a surprisingly small contribution from the Pt $5d_{z^2}$ orbital (27%), and the unpaired "metal" electron is essentially delocalized on the axial ligand. Furthermore, the large intersphere contribution to this MO confirms the extent of this delocalization. The related bonding MO is $5a_1$, which provides essentially the metal–oxygen σ-bonding interaction, with a nonnegligible participation of the Pt 6s AO. The 5e and 6e MO's are respectively bonding and antibonding with regard to the π metal–oxygen interactions, while the former MO supplies also most of the π metal–chlorine antibonding interactions. The related Pt–Cl π bonding is provided by the 2e MO.

The population analysis, for the entity $PtCl_4(OH)^{2-}$, leads to the following charge distribution: $Pt[5d^{7.75}(d\sigma^{2.21}d_\pi^{5.54})-6s^{0.48}6p^{0.45}5f^{0.15}]Cl^{-0.63}OH^{-0.63}$. The Pt net charge is +1.17. With respect to the ionic model of a Pt^{3+} cation surrounded by five anions, the ligand spheres have lost 1.21 e to the benefit of the Pt $5d_\sigma$ orbitals, while a simultaneous back-donation of 0.46 e has decreased the population of the metal $5d_\pi$ orbtials.

The occupation of the σ-antibonding HOMO implies a substantial electronic repulsion between the metal and the axial ligand. This effect must weaken the Pt–O bond and thus lead to its elongation, although it does not correspond to a true Jahn–Teller deformation. The evolution of the upper valence energy levels, with respect to the Pt–O elongation (model B), is illustrated in Figure 1. This diagram shows that the levels involving only the equatorial chlorine and platinum orbitals remain nearly unchanged. In contrast, the energies of the $6a_1$ and $5a_1$ MO's (σ-antibonding and σ-bonding Pt–O interactions) are respectively lowered and

(9) Troemel, M.; Lupprich, E. *Naturwissenschaft* **1973**, *60*, 351.
(10) Dickinson, R. G. *J. Am. Chem. Soc.* **1922**, *44*, 2404.
(11) Watson, R. E. *Phys. Rev.* **1958**, *111*, 1108.
(12) (a) Schwartz, K. *Phys. Rev. B: Solid State* **1972**, *5*, 2466. (b) Schwartz, K. *Theor. Chim. Acta* **1974**, *34*, 225.
(13) Slater, J. C. *Adv. Quantum Chem.* **1972**, *6*, 1.
(14) Waltz, W. L.; Lilie, J.; Walters, R. T.; Woods, R. J. *Inorg. Chem.* **1980**, *19*, 3284.

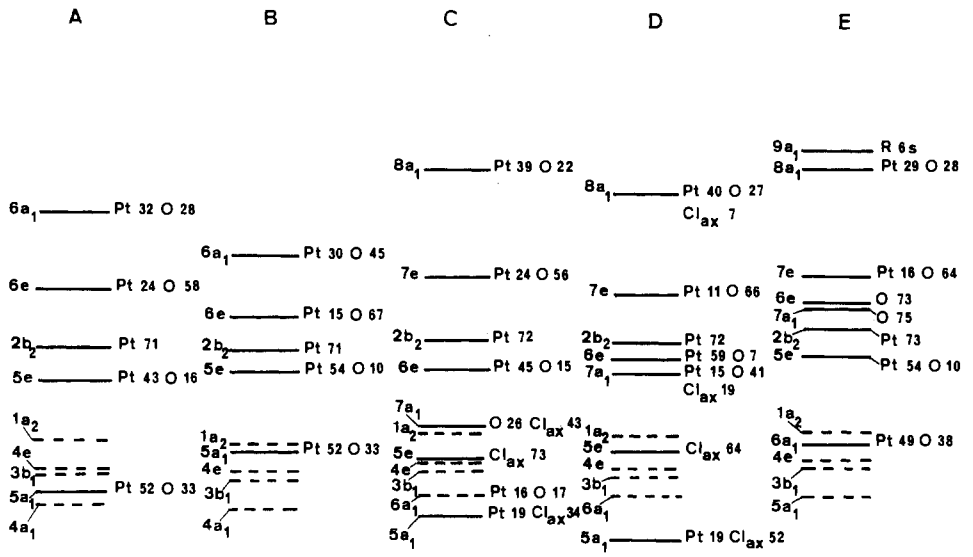

Figure 1. Ground-state energy levels: A, $PtCl_4O^{3-}$ (Pt–O = 3.855 au); B, $PtCl_4O^{3-}$ (Pt–O = 4.388 au); C, $PtCl_5O^{4-}$ (Pt–O = 3.855 au; Pt–Cl_{ax} = 5.388 au); D, $PtCl_5O^{4-}$ (Pt–O = 4.388 au; Pt–Cl_{ax} = 4.788 au); E, $PtCl_4O_2^{5-}$ (Pt–O = 4.388 au). The Pt, O, and Cl_{ax} major contributions are indicated in percent. Dotted lines are used for levels having preponderantly Cl_{eq} character.

Table II. Electronic Energy Levels[a] and Charge Distribution for $PtCl_4O_2^{5-}$

MO	energy, Ry	Pt								Cl_{eq}			O			int	out
		s	p_z	$p_{x,y}$	d_{z^2}	$d_{x^2-y^2}$	d_{xy}	$d_{xz,yz}$	f	s	p_σ	p_π	s	p_σ	p_π		
$9a_1$	−0.060				9					4				8		17	62
$8a_1$	−0.082				29						4		2	26		15	24
7e	−0.225							16							64	18	2
6e	−0.257										1				73	23	3
$7a_1$	−0.263		4						1			2		75		14	4
$2b_2$	−0.294						73					17				9	1
5e	−0.327							54				25			10	11	
$1a_2$	−0.428											90				9	1
$6a_1$	−0.442	7			42									38		12	1
4e	−0.465			1					1		86					9	3
$3b_1$	−0.473											86				13	1
$5a_1$	−0.512		1									78		2		17	2
3e	−0.539										83					8	3
2e	−0.542							21				60			2	16	1
$1b_2$	−0.591						19					64				16	1
$2b_1$	−0.646					37				1	60						2
$4a_1$	−0.664	13			11					2	70					2	2
$3a_1$	−1.289		1										90			8	1
$2a_1$	−1.293				2					3			88			7	
1e	−1.345			2						94						3	1
$1b_1$	−1.346					4				94						2	
$1a_1$	−1.380	3			1					89	1		2			4	

[a] The highest occupied level is $8a_1$, which accommodates one electron.

increased. The same feature, but less pronounced, is to be noticed for the π 6e and 5e MO's. It is thus clear that the CT transition energies involving the HOMO will be appreciably decreased when the Pt–O bond is elongated. This effect has already been evaluated in the case of the Jahn–Teller tetragonal distortion of an octahedral d^7 complex.[4]

To analyze the influence on the absorption spectrum of additional chlorine anions in the experimental situations, $PtCl_5O^{4-}$ structures have been calculated to model a $PtCl_5OH^{3-}$ complex (i) with inclusion of a sixth axial weakly coordinating Cl ligand (model C) and (ii) with elongated Pt–O and Pt–Cl_{ax} bond lengths (model D). The calculated upper energy levels of these models are shown in Figure 1 as C and D. With respect to $PtCl_4O^{3-}$, all the valence levels are shifted slightly upward; however, their relative positions are maintained, except for those involving the Pt–O σ interactions. Although the participation of the additional axial chlorine is small, it does induce an increase in the $6a_1$–$8a_1$ energy separation. Moreover, three additional MO's are now to be taken into account. One is the nonbonding 5e MO, characteristic of the axial Cl $3p_\pi$ orbitals. The other two are $5a_1$ and $7a_1$. Both correspond mainly to the contribution of the axial ligand p_σ orbitals, combined with moderate participations of the Pt $5d_{z^2}$ orbital. The $5a_1$ MO provides principally the σ-bonding interactions between the metal and the additional chlorine. On the other hand, the weak Pt and Cl_{eq} contributions to $7a_1$ (12% and 8%, respectively, for model C) confer a major nonbonding character on this MO, mainly localized on the axial ligands. The main feature attached to a six-coordinated complex is thus the presence of a quasi-nonbonding σ-type MO, characteristic of the axial ligands. Its energy is situated in the upper region of the valence band, distinctly higher than the energy of the σ Pt–axial ligand bonding MO of a pentacoordinated complex. When the axial chlorine is set closer to Pt, as in model D, the $7a_1$ MO is still shifted upward. In fact, this a_1 MO in C_{4v} symmetry (a_{2u} in D_{4h}) involves the pair of axial ligands and is derived from the one component spanning z of a t_{1u} nonbonding MO in O_h. The presence of this additional level of σ type will be of major importance for the assignment of the CT spectra of the observed transients.

(2) $PtCl_4O_2^{5-}$. The valence levels of this structure (model E), including elongated Pt–O bond lengths, are reported in Table II. The results are presented according to the C_{4v} symmetry for easier

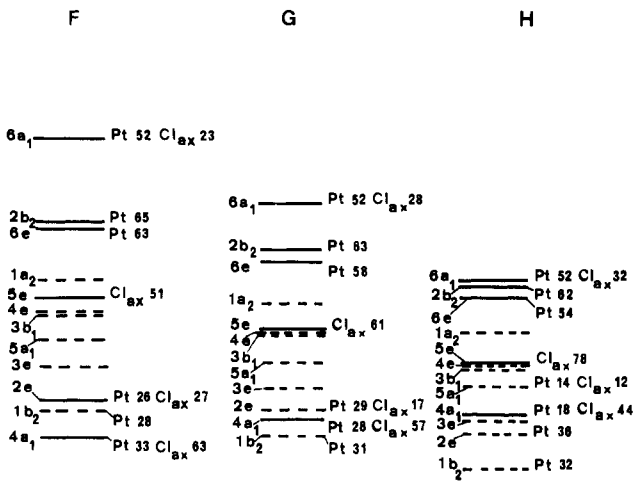

Figure 2. Ground-state energy levels of $PtCl_5^{2-}$, without (F) and with Pt–Cl_{ax} bond length elongations (G, 0.4 au; H, 1.0 au). Pt and Cl_{ax} major contributions are indicated in percent. Dotted lines are used for levels having a preponderantly Cl_{eq} character.

comparison with those for $PtCl_4O^{3-}$. The unpaired electron, populating the σ-antibonding HOMO $8a_1$, is largely delocalized over the whole complex. Indeed, the charge participation of the extramolecular region to the HOMO amounts to 24%. The analysis of the fractional charge contained in the outer-sphere contribution leads to the idea that this MO has a notable amount (15%) of Pt 6s Rydberg character. In fact, a valence–Rydberg mixing occurs, caused by the close energies of the Pt 6s Rydberg orbital and of the σ-antibonding Pt–O MO. Some Rydberg character is thus gained by the HOMO, while some valence character is gained by the Pt 6s Rydberg orbital ($9a_1$). The energy gap between $8a_1$ and $9a_1$ is calculated to be very small (0.3 eV). In fact, the presence of low-lying Rydberg orbitals (Pt 6p) has already been mentioned in the case of $PtCl_4^{2-}$[16,19] to interpret its high-intensity spectrum, although other assignments have been proposed.[15,17,18] The $6a_1$ MO is strongly σ bonding, with almost equal Pt and O participations. The 5e and 7e MO's show the weak π-bonding and π-antibonding Pt–O interactions, respectively.

A comparison with the valence levels of the previous models is presented in Figure 1. With respect to the hexacoordinated $PtCl_5O^{4-}$ model, the relative positions of the MO's involving the Pt–Cl_{eq} interactions ($3b_1$, 4e, $1a_2$, $2b_2$, 7e) are roughly conserved. In the same way, the 7e and $8a_1$ MO's, in which the axial Cl of $PtCl_5O^{4-}$ does not participate (respectively 0% and 4% Cl_{ax} participation), are found at comparable energies, with similar weakly antibonding π (7e) or σ ($8a_1$) Pt–O character. The σ-bonding $5a_1$ MO of $PtCl_5O^{4-}$ is shifted upward, due to the replacement of Cl by O (it becomes $6a_1$). In the same way, the nonbonding Cl $3p_\pi$ 5e MO of $PtCl_5O^{4-}$ is replaced, at higher energy, by the nonbonding O $2p_\pi$ 6e MO. The energy of $7a_1$, a weak Pt–O and Pt–Cl σ-bonding MO, is also increased, due to the loss of most of the Pt contribution and the replacement of Cl_{ax} by O. As stated previously, the presence of this nonbonding σ MO, which is related to the presence of a pair of axial ligands, is of major importance for the interpretation of the CT absorption spectra.

(3) $PtCl_5^{2-}$. The calculated electronic structure of $PtCl_5^{2-}$ (C_{4v}) without Pt–Cl_{ax} elongation (model F) is reported in Table III. The $6a_1$ HOMO corresponds to strong antibonding interactions between the Pt $5d_{z^2}$ and Cl_{ax} $3p_z$ orbitals. In contrast with that of $PtCl_4O^{3-}$, the metal participation is substantial, leading to an approximately equal contribution of the unpaired electron to the Pt and axial chlorine charges. A comparison of the valence energy levels of $PtCl_4O^{3-}$ (Figure 1A) and $PtCl_5^{2-}$ (Figure 2F) shows the permanence of the relative positions of the levels involving the planar $PtCl_4$ part of the complex. The $2b_2$ and 6e levels, issuing from t_{2g} (O_h), are closer in $PtCl_5^{2-}$ due to the same nature of the axial and equatorial ligands. For the same reason, the energy of the nonbonding 5e MO, characteristic mainly of the Cl_{ax} $3p_\pi$ orbitals and related to 6e in $PtCl_4O^{3-}$, becomes closer to the energies of the π-nonbonding MO's involving the Cl_{eq} ligands ($1a_2$, 4e, $3b_1$).

As illustrated in Figure 2, the major trend due to the Pt–Cl_{ax} elongation (models G and H) is the decrease in the energy separation between the related bonding and antibonding σ MO's. The destabilization of the former and the simultaneous stabilization of the latter are a consequence of the decreased electronic repulsion. Moveover, as the Pt–Cl_{ax} bond length is elongated, the Pt 5d levels (6e, $2b_2$, $6a_1$) become more compacted and the $4a_1$ MO is shifted upward. At the same time, it changes from a bonding Pt–Cl_{ax} character (model F) to a nonbonding Cl_{ax} one (model H).

Calculated CT Spectra and Comparison with Experiment

The experimental absorption spectra of the transients show predominantly one intense band. Their molar extinction coefficients have been evaluated at about 3000–4000 M^{-1} cm^{-1} for the 450- and 410-nm bands[5,6] and at about 9000 or 7000 M^{-1} cm^{-1} for the intense absorption near 260[8] or 290 nm.[7] The intensities of these bands are indicative of CT transitions that are allowed by the symmetry selection rules. The corresponding calculated transitions of $PtCl_4O^{3-}$, $PtCl_5O^{4-}$, and $PtCl_4O_2^{5-}$ are given in Table IV, while those for $PtCl_5^{2-}$ and $PtCl_6^{3-}$, including previous results on axially distorted $PtCl_6$ octahedra[4] are presented in Table V.

As expected from the energy level diagrams, the elongations of the axial Pt–O and Pt–Cl bond lengths imply a substantial red shift for all of the calculated CT transitions. The presence of a sixth coordinating ligand in $PtCl_5O^{4-}$ results in a blue shift of the CT transitions from the ligand π MO's to the metal $5d_{z^2}$ orbital. The $7a_1 \rightarrow 8a_1$ transitions occur at a lower energy than the related $5a_1 \rightarrow 6a_1$ transition in $PtCl_4O^{3-}$, but this red shift only amounts to about 3000 cm^{-1}. Due to the presence of six chloride ligands, the calculated spectrum of $PtCl_6^{3-}$, including two elongated Pt–Cl_{ax} bonds (D_{4h} symmetry), is substantially different from that of its pentacoordinated homologue (C_{4v} symmetry). However, the CT transitions from the Cl_{ax} $3p_\sigma$ MO to the metal $5d_{z^2}$ orbital have similar calculated energies for both structures.

Before comparing the calculated results with the experimental peak positions, it is necessary to select from all the calculated transitions those that could have appropriate intensities. If we apply the qualitative rule stated by Day and Sanders,[20] then the only intense CT transitions are those that have a transition moment polarized in the same direction as the electron flow resulting from the CT act. In the present case of C_{4v} structures, the spin-allowed transitions from the $^2A_1$ ground state to $^2A_1$ excited states are the only ones that could yield intense absorptions (electrons transferred along the z axis), since we consider the CT transitions involving the singly occupied HOMO. In the same context, only the $^2A_{1g} \rightarrow {}^2A_{2u}$ transitions in D_{4h} symmetry need to be considered. To assign the experimental absorption bands to specific structures, we thus need to account only for the $a_1 \rightarrow a_1$ or $a_{2u} \rightarrow a_{1g}$ transitions in C_{4v} or D_{4h} symmetry, respectively.

We will first consider the experimental spectrum observed in neutral aqueous solutions, which consists of a single 450-nm peak, observed at the end of the pulse. It corresponds to a Pt(III) species directly obtained from the reaction between Pt(II) and the OH radical.

For the $PtCl_4O^{3-}$ model (Figure 1A,B), the $5a_1 \rightarrow 6a_1$ transition is calculated to be at 240 and 340 nm for the nonelongated and elongated Pt–O length cases, respectively. These calculated wavelengths are well removed from the experimental absorption at 450 nm, and as such, the $PtCl_4O^{3-}$ model (or $PtCl_4OH^{3-}$) seems inappropriate. In the same way, the $PtCl_5O^{4-}$ structure (Figure 1C,D), including a sixth weakly coordinating chlorine, cannot be

(15) Basch, H.; Gray, H. B. *Inorg. Chem.* **1967**, *6*, 365.
(16) Cotton, F. A.; Harris, C. B. *Inorg. Chem.* **1967**, *6*, 369.
(17) Jørgensen, C. K. *Prog. Inorg. Chem.* **1970**, *12*, 130.
(18) Elding, L. I.; Olsson, L. F. *J. Phys. Chem.* **1978**, *82*, 69.
(19) Chermette, H.; Goursot, A. *Can. J. Chem.*, in press.
(20) Day, P.; Sanders, N. *J. Chem. Soc. A* **1967**, 1536.

Table III. Electronic Energy Levels[a] and Charge Distribution for $PtCl_5^{2-}$

MO	energy, Ry	Pt								Cl_{eq}			Cl_{ax}			int	out
		s	p_z	$p_{x,y}$	d_{z^2}	$d_{x^2-y^2}$	d_{xy}	$d_{xz,yz}$	f	s	p_σ	p_π	s	p_σ	p_π		
$4b_1$	−0.150					51				4	32					8	5
$6a_1$	−0.279	2	3		47						5	3	1	22		15	2
$2b_2$	−0.396						65					25				9	1
6e	−0.407							63				23			5	8	1
$1a_2$	−0.480											90				9	1
5e	−0.504							1	1		9	27			51	10	1
4e	−0.519			1					1		19	66			2	10	1
$3b_1$	−0.525											87				12	1
$3a_1$	−0.561		1		3							78		2		15	1
3e	−0.597			6				4		1	55	25				7	2
2e	−0.645			1				25			4	28			27	14	1
$1b_2$	−0.660						28					57				14	1
$4a_1$	−0.697	4	2		27							2	1	62		3	1
$2b_1$	−0.734					42				2	55						1
$3a_1$	−0.741	15			11					3	67					2	1
1e	−1.403			2						95						3	
$1b_1$	−1.406					5				94						1	
$2a_1$	−1.413		1		3					27			67			2	
$1a_1$	−1.448	5								64			27			3	

[a] The highest occupied level is $6a_1$, which accommodates one electron.

Table IV. Calculated CT Transitions (nm) for the $PtCl_4O^{3-}$, $PtCl_5O^{4-}$, and $PtCl_4O_2^{5-}$ Models

transition	preponderant character of the originating MO	$PtCl_4O^{3-}$ without Pt–O elongation [A]	$PtCl_4O^{3-}$ with Pt–O elongation [B]	transition	preponderant character of the originating MO	$PtCl_5O^{4-}$ with a weakly coordinating Cl_{ax} [C]	$PtCl_5O^{4-}$ with Pt–O and Pt–Cl_{ax} elongation [D]	$PtCl_4O_2^{5-}$ with Pt–O elongation [E]
$6e \rightarrow 6a_1$	O (π)	850	1080	$7e \rightarrow 8a_1$	O (π)	600	635	615
$5e \rightarrow 6a_1$	M ($d\pi$) + Cl_{eq} (π)	360	504	$6e \rightarrow 8a_1$	M (d_π) + Cl_{eq} (π) [C, D] O (π) [E]	340	410	506
$4e \rightarrow 6a_1$	Cl_{eq} (σ)	250	280	$7a_1 \rightarrow 8a_1$	O (σ) + Cl_{ax} (σ) [C, D] O (σ) [E]	260	360	460
$5a_1 \rightarrow 6a_1$	O (σ) + M (d_σ)	240	340	$5e \rightarrow 8a_1$	Cl_{ax} (π) [C, D] M (d_π) + Cl_{eq} (π) [E]	235	260	355
				$4e \rightarrow 8a_1$	Cl_{eq} (σ) [C, D, E]	220	230	220
				$6a_1 \rightarrow 8a_1$	Cl_{eq} (π) + O (σ) [C, D] M (d_σ) + O (σ) [E]	207	220	240

Table V. Calculated CT Transitions (nm) for the $PtCl_5^{2-}$ and $PtCl_6^{3-}$ Models

transition	preponderant character of the originating MO	$PtCl_5^{2-}$ (C_{4v}) without Pt–Cl_{ax} elongation [F]	$PtCl_5^{2-}$ (C_{4v}) with Pt–Cl_{ax} elongation 0.4 au [G]	$PtCl_5^{2-}$ (C_{4v}) with Pt–Cl_{ax} elongation 1 au [H]	transition	preponderant character of the originating MO	$PtCl_6^{3-}$ (D_{4h}) with Pt–Cl_{ax} elongation 0.2 au [I]	$PtCl_6^{3-}$ (D_{4h}) with Pt–Cl_{ax} elongation 0.4 au [J]
$5e \rightarrow 6a_1$	Cl_{ax} (π)	355	455	593	$3a_{2u} \rightarrow 5a_{1g}$	Cl_{ax} (σ)	266	318
$4e \rightarrow 6a_1$	Cl_{eq} (π)	320	400	540	$4e_u \rightarrow 5a_{1g}$	Cl_{ax} (π)	259	302
$5a_1 \rightarrow 6a_1$	Cl_{eq} (π)	280	370	560	$3e_u \rightarrow 5a_{1g}$	Cl_{eq} (π)	250	276
$3e \rightarrow 6a_1$	Cl_{eq} (σ)	255	304	380	$2a_{2u} \rightarrow 5a_{1g}$	Cl_{eq} (π) + Cl_{ax} (σ)	207	214
$4a_1 \rightarrow 6a_1$	Cl_{ax} (σ) + M (d_σ)	210	284	450	$2e_u \rightarrow 5a_{1g}$	Cl_{eq} (σ)	203	235

related to the experimental spectrum, since its lowest CT transition is at 260 nm and this position could not be shifted further than 380 nm even with substantial elongation of the Pt–O bond.

Both of these structures are thus inconsistent with the experimentally observed spectrum. In contrast, the six-coordinated $PtCl_4O_2^{5-}$ model (Figure 1E) presents a CT transition ($7a_1 \rightarrow 8a_1$), which is calculated at 460 nm. As mentioned previously, this O $p_\sigma \rightarrow$ Pt $5d_{z^2}$ transition results from the presence of an additional pure-ligand σ MO, which is related to the presence of *two* axial ligands. The $6a_1 \rightarrow 8a_1$ transition, which has a mixed d–d and CT character, is calculated at 240 nm. Unfortunately, its potential presence is obscured in experiments by the intense absorption of the reactant $PtCl_4^{2-}$ in this region.

We now examine the Pt(III) models that most likely pertain to the results obtained in neutral and acidic $PtCl_4^{2-}$–Cl^- systems. In this situation, Pt(II) appears to be oxidized by the Cl_2^- species and the resulting Pt(III) transient(s) exhibits an intense absorption band with a peak at 260–290 nm. It is shown in Table V that the C_{4v} $PtCl_5^{2-}$ model (Figure 2F,G,H) has two CT transitions of a_1–a_1 type. The first one ($5a_1 \rightarrow 6a_1$) involves the Cl_{eq} $3p_\pi$ orbitals as the electron donor, the second one ($4a_1 \rightarrow 6a_1$) is associated with mixed Cl_{ax} $3p_\sigma$ and Pt $5d_{z^2}$ interactions. It is at first sight surprising that the former transition could carry a substantial intensity since the Pt $5d_{z^2}$ and Cl_{eq} $3p_\pi$ orbitals must have a small overlap. This $5a_1$ MO is derived from a t_{1u} MO (O_h) and thus corresponds to an odd linear combination of Cl_{eq} $3p_z$ orbitals. Nevertheless, Jørgensen[21] has pointed out that this type of ligand $\pi \rightarrow$ M $5d_\sigma$ CT transition is related to broad intense bands, such as is the case for $PtCl_6^{2-}$.[3] It appears from these results that only the $PtCl_5^{2-}$ structure without Pt–Cl_{ax} elongation can fit the experimental spectrum (no intense absorptions above 280 nm). However, it seems unlikely that the population of the strong antibonding $6a_1$ MO does not imply a much looser bonding between the metal and the axial ligand than in the case of a Pt^{IV}–O bond (d^6 complex). According to our previous results,[4] a D_{3h} $PtCl_5^{2-}$ structure must have three intense CT transitions. They would lead to two absorption bands at about 260 and 320 nm, instead of the one, as is observed.

We are thus led to consider, for this transient also, the possibility of a six-coordinated structure such as $PtCl_6^{3-}$ or $PtCl_5O^{4-}$. Examination of Table IV shows that the $PtCl_5O^{4-}$ structure, *without* Pt–O elongation and with a weakly coordinating chlorine (model C), should have an intense CT transition at 260 nm. If one includes moderately elongated Pt–Cl_{ax} and Pt–O bond lengths (model D), then the calculated CT transitions (360 and 220 nm) fall outside the experimentally observed range. As with the $PtCl_5^{2-}$ case, the $PtCl_5O^{4-}$ structure (model C) appears inadequate, because of its lack of Pt–O elongation with respect to the standard value of a Pt^{IV}–O bond length.

The results presented in Table V do indicate that a $PtCl_6^{3-}$ species with moderate Pt–Cl_{ax} bond elongation (0.2 or 0.3 au) can exhibit an intense CT transition near 270–290 nm.

On the basis of our calculations and the experimental observations, the most consistent picture of the reaction of OH with $PtCl_4^{2-}$ appears to involve OH addition:

$$PtCl_4^{2-} + OH \xrightarrow{H_2O} PtCl_4(OH)(H_2O)^{2-} \text{ or } PtCl_4(OH)_2^{3-}$$

It is difficult to discern if the generated Pt(III) species is the hydroxo–aquo form or the dihydroxo-substituted case, since the acid dissociation constant of the aquo complex is unknown. However, the detection of the 450-nm peak appears to be very sensitive to the presence of both acid and base, and this strongly suggests a $PtCl_4(OH)(H_2O)^{2-}$ structure.

EXAFS measurements on the Jahn–Teller $Cu(H_2O)_6^{2+}$ complex have shown that the axial Cu–O bond length is elongated by about 0.65 Å.[22] In this case, the very loosely bonded axial ligands are substituted very rapidly, particularly by a water solvent molecule. In our case, we can thus imagine the rapid conversion from $PtCl_4(OH)(H_2O)$ to a longer-lived transient:

$$PtCl_4(OH)(H_2O)^{2-}\ (450\text{ nm}) \xrightarrow{k = 2 \times 10^5\ s^{-1}} PtCl_4^-\text{ type (410 nm)}$$

This latter step may well be catalyzed by H^+ and OH^-, so it would not be seen in acid or concentrated base, which is consistent with the observations.[5,7]

As reported previously,[4] the complex absorbing at 410 nm may be the square-planar $PtCl_4^-$ complex itself or a square-planar structure with weakly coordinating ligands in apical positions. The route to the long-lived transient of $PtCl_4^-$ type could be simply the loss of one and then both axial ligands.

For the transient species observed in pulse radiolysis of $Pt^{II}Cl_4^{2-}$ in the presence of the Cl_2^- radical, our calculations suggest a $PtCl_6^{3-}$ structure with moderate elongations of the Pt–Cl_{ax} bond lengths (0.2–0.3 Å) with respect to a standard Pt–Cl bond value of 2.04 Å. In this case, the reaction of Cl_2^- with $PtCl_4^{2-}$ could be written

$$(PtCl_4\cdots Cl\text{–}Cl^{-*}) + Cl^- \rightarrow PtCl_6^{3-} + Cl^{-*}$$

The final product $PtCl_6^{3-}$ may be obtained in two steps

$$PtCl_4^{2-} + Cl\text{–}Cl^- \xrightarrow{H_2O} PtCl_5(H_2O)^{2-} + Cl^-$$

$$PtCl_5(H_2O)^{2-} + Cl^- \underset{}{\overset{HCl}{\rightleftharpoons}} PtCl_6^{3-}$$

the second reaction being strongly displaced to the right in the acidic medium. We may thus summarize our calculated results by writing the following reactions:

$$Pt^{II}Cl_4^{2-} + OH\cdot \xrightarrow{H_2O} PtCl_4(OH)(H_2O)^{2-} \text{ or } PtCl_4(OH)_2^{3-}$$

$$Pt^{II}Cl_4^{2-} + Cl_2^- \xrightarrow{Cl^-} PtCl_6^{3-}$$

As a final remark, it must be pointed out that the analysis of the calculated CT spectra of penta- and hexacoordinated Pt(III) structures has led to the conclusion that only hexacoordinated models could yield the agreement with the experimental spectra. This result is consistent with the proposal that the vacancy of the sixth coordinating position in d^7 complexes destabilizes C_{4v} models compared with D_{4h} or O_h structures.

Acknowledgment. Part of these calculations have been performed at the Centre de Calcul CNRS, Strasbourg-Cronenbourg. Financial support of NATO is gratefully acknowledged (Project No. 018.81). The assistance to W.L.W. has been kindly provided by the Natural Sciences and Engineering Research Council of Canada.

(21) Jørgensen, C. K. *Mol. Phys.* **1959**, *2*, 309.

(22) Sham, T. K.; Hastings, J. B.; Perlman, M. L. *Chem. Phys. Lett.* **1981**, *83*, 391.